fire

MDPI

Article

Deep Learning-Based Remote Sensing Image Analysis for Wildfire Risk Evaluation and Monitoring

Shiying Yu [1,*] and Minerva Singh [2,3]

[1] Department of Earth Science and Engineering, Imperial College London, London SW7 1NE, UK
[2] Centre for Environmental Policy, Imperial College London, London SW7 1NE, UK
[3] Nature Based Solutions Initiative (NBSI), School of Geography and Environment, Oxford University, Oxford SW7 2UA, UK
* Correspondence: shiying.yu23@imperial.ac.uk

Abstract: Wildfires have significant ecological, social, and economic impacts, release large amounts of pollutants, and pose a threat to human health. Although deep learning models outperform traditional methods in predicting wildfires, their accuracy drops to about 90% when using remotely sensed data. To effectively monitor and predict fires, this project aims to develop deep learning models capable of processing multivariate remotely sensed global data in real time. This project innovatively uses SimpleGAN, SparseGAN, and CGAN combined with sliding windows for data augmentation. Among these, CGAN demonstrates superior performance. Additionally, for the prediction classification task, U-Net, ConvLSTM, and Attention ConvLSTM are explored, achieving accuracies of 94.53%, 95.85%, and 93.40%, respectively, with ConvLSTM showing the best performance. The study focuses on a region in the Republic of the Congo, where predictions were made and compared with future data. The results showed significant overlap, highlighting the model's effectiveness. Furthermore, the functionality developed in this study can be extended to medical imaging and other applications involving high-precision remote-sensing images.

Keywords: wildfire; deep learning; remote sensing; multivariate data; generative adversarial network

Received: 23 October 2024
Revised: 6 December 2024
Accepted: 29 December 2024
Published: 5 January 2025

Citation: Yu, S.; Singh, M. Deep Learning-Based Remote Sensing Image Analysis for Wildfire Risk Evaluation and Monitoring. *Fire* **2025**, *8*, 19. https://doi.org/10.3390/fire8010019

1. Introduction

Forest fires not only cause sustainability concerns by destroying vast areas of trees, plants, and wildlife, but they also endanger the safety of forest inhabitants and delay social and economic progress [1–4]. Furthermore, they can have long-term implications for soil quality, water supplies, and ecological stability if allowed unregulated for extended periods of time. In addition, wildfires are significant contributors to air pollution, releasing large quantities of carbon dioxide (CO_2) along with other harmful pollutants such as black carbon, volatile organic compounds (VOCs), and nitrogen oxides (NO_x) [5–7]. These emissions increase global warming and contribute to poor air quality, which is linked to severe health issues, including respiratory diseases, cardiovascular problems, increased mortality rates, and so on. For example, according to reports from the World Health Organisation (WHO), exposure to smoke from wildfires increases the risk of heart disease, stroke, and chronic respiratory problems [8–10]. Early detection is crucial due to the swift propagation and devastating capacity of wildfires. Studies have shown that to effectively prevent a fire from spreading uncontrollably, it must be detected within six minutes, a benchmark set by the National Fire Danger Rating System (NFDRS) [11–13]. This stresses the urgent need for an

efficient and reliable classification network that can identify fires early and as previously stated, reduce the disastrous effects of fires on the environment and public health [14].

According to the results of an exploration of the literature, western US wildfires were the topic of 15% of research publications, despite only accounting for 0.5% of the global area burnt [15,16]. In contrast, research on wildfire-prone Siberia and Africa is scarce. This may be due to the lack of adequate financial support, the difficulty of collecting suitable data, and the employment of traditional methods of fire detection and monitoring, such as human-based observation. This is because human-based observation has low efficiency and practicality, low fire localizing accuracy, and long detection delay [14,17,18]. Also, this system cannot be used for other purposes, unlike other detection systems, which can be re-programmed for other applications. On the upside, human-based observation is low in cost as well as low in faulty alarm repetition. However, recent advancements in deep-learning techniques for fire detection and monitoring offer a more flexible process and accurate data than traditional methods. For example, UAV-based detection and transfer learning with improved Faster RCNN has achieved 93.7% accuracy [19–21], while segmentation methods like SqueezeNet on images have achieved 94.2% accuracy [22–24]. For satellite image detection and segmentation, YOLOv5S and MobileNetV3 achieved 90.5% accuracy [25–27], and DCNN image segmentation and classification have shown the highest accuracy of 99.9% [28–30]. Forest fire detection has improved, with CNN-based image processing methods reaching 96% accuracy [31,32].

Based on the techniques mentioned above, this study discovered that as deep learning methods are merged with several disciplines, the growing number of linked works in the remote sensing and wildfire domains has brought attention to their significance. These deep learning models have proven to be feasible in real-world applications in addition to exhibiting improved accuracy. However, this study also revealed several issues that still need to be resolved in this field. To start, the unbalanced nature of the study area has resulted in wildfires in the Africa region, which have hampered regional growth and claimed lives. Second, while remotely sensed data have received minimal attention, the majority of research data are image-based. This could be because data from remote sensing typically spans several bands and includes intricate and extensive information. This means that not only is it more data-intensive and computationally demanding, but it is also more challenging to interpret. Thirdly, and perhaps most concerningly, there has not been much research conducted to date, despite the significant current demand for fire prediction and monitoring models that can react to real-time remotely sensed data. This might be because, aside from certain government agencies that have access to data and computational resources, research teams typically struggle with the rigorous criteria for modeling and pre-processing data sets. It is fascinating to observe how these issues are attempted to be resolved, and solutions are greatly needed.

The goal of this work is to utilize real-time remotely sensed data through advanced, yet appropriate, pre-processing techniques integrated with deep learning-based models, building on existing research. The dataset taken into account for this research is from the Republic of the Congo because this country is facing the highest incidence of wildfires among all countries globally, with very little research in this direction to try to address the research imbalance mentioned above. This research has selected models like U-Net and CNN that are appropriate for processing time series for prediction and classification in a short time. This is necessary due to the difficult task of pre-processing real-time remote sensing data and the requirement of generating complements for missing data in conjunction with Generative Adversarial Network (GAN) models [33,34]. The objective is to create and evaluate a technical path for wildfire forecasting that uses remotely sensed data with a low overhead cost and a respectable level of accuracy in an attempt to address

the previously mentioned processing deficiency problem for processing remotely sensed data. The goal of this research is to experiment with novel application solutions that may be investigated and further integrated in the future.

2. Materials and Methods

2.1. Study Area

To address the previously noted research disparity, this study chose a region situated in the central region of the Democratic Republic of the Congo, encompassing the Kasai and Sankuru provinces. It ranges from the tropical rainforest of the north to a more densely populated agricultural savannah area in the south. The study area in totality encompasses about 72,000 km^2 of diverse topography and ecosystems within the tropical climate zone. It has a dry season from May to September and a wet season from October to April. Biogeographically, this part of the region is rich, and in its northern part, which forms part of the Congo Basin, there are the world's second-largest tropical rainforests, which play an important role in global carbon storage. In recent years, for the northern area, logging activity has increased in these forested areas, thereby leading to habitat fragmentation and environmental degradation; for the southern area, the landscape has changed into savannah and secondary forests, where human activities are more intense. These include smallholder agriculture, animal husbandry, deforestation, and land clearing, hence creating an environment highly prone to fire outbreaks [35–37].

The region experiences recurring wildfires, particularly in the southern area, due to significant agricultural activities. Wildfires typically arise in the arid season and are mostly a result of slash-and-burn agricultural methods. Approximately 70% of the total area burned worldwide each year is attributed to Sub-Saharan Africa, with the Democratic Republic of the Congo being one of the most severely impacted areas. As depicted in Figure A1, although the African continent has one of the highest wildfire rates worldwide, it still lacks an efficient fire management system. Hence, the incorporation of this region as a study area is highly logical, benefiting both the environment and human welfare.

2.2. Data Source

2.2.1. VIIRS Fire Dataset

The fire monitoring data were taken in this work using a merged dataset from NASA (National Aeronautics and Space Administration) LANCE SNPP VIIRS C2 [38] and NASA LANCE NOAA-20 VIIRS C2 [39], as shown in Table 1. These two datasets provide global coverage and have continuous temporal coverage starting from 3 September 2023 to the present, with daily updates. These data and images are being collected in near real-time with a latency of only 3 h, minimizing detection delay. Moreover, the dataset sources have fine spatial resolution and improved mapping, especially for larger fire perimeters. The VIIRS (Visible Infrared Imaging Radiometer Suite) sensor is a critical instrument onboard both the Suomi National Polar-orbiting Partnership (SNPP) and NOAA-20 satellites that helps to determine fire intensity on the Earth's surface by detecting hotspots and thermal anomalies and measuring Bright-ti4 (brightness temperature), allowing for the assessment of fire intensity. VIIRS is designed to provide comprehensive data for various environmental applications, leveraging its advanced capabilities in capturing visible, near-infrared, and shortwave infrared spectral radiances. This suite consists of 22 spectral bands, which range from 0.41 to 12.5 µm, allowing for detailed observations of the Earth's surface and atmosphere, including land, ocean, and atmospheric phenomena. The dataset also includes a confidence metric linked to the number of fire detections, which helps to quantify the reliability of these detections. Additionally, the diurnal band is used to investigate the differences between daytime and nighttime fire occurrences, providing insights into diurnal

fire dynamics. This globally integrated, high-frequency, all-weather dataset is used to detect fire events in the study area and analyze their spatial distribution, offering essential support for real-time fire risk assessments.

Table 1. Overview of satellite datasets.

Dataset	NOAA-20 VIIRS C2	SNPP VIIRS C2	Sentinel-1 GRD	Sentinel-2 SR Harmonized
Provider	NASA	NASA	European Space Agency (ESA)	European Space Agency (ESA)
Resolution	375 m	375 m	10 m	10 to 60 m
Area	Global	Global	Global	Global
Time	From 8 October 2023 to present	From 3 September 2023 to present	From 3 October 2014 to present	From 28 March 2017 to present
Update	Daily	Daily	Daily	Daily
Band Info.	Bright-ti4: 250–400 K, brightness temperature of fire pixels; Confidence: 0–2 (low, nominal, high); DayNight: 1 = Daytime fire, 0 = Nighttime fire	Bright-ti4: 250–400 K, brightness temperature of fire pixels; Confidence: 0–2 (low, nominal, high); DayNight: 1 = Daytime fire, 0 = Nighttime fire	VV, VH: 10 m, dB range −50 to 1, VV (single co-polarization), VH (dual-band cross-polarization)	B4, B8: 10 m, NIR, 835.1 nm (S2A)/833 nm (S2B); SCL: 20 m, Scene Classification Map, values 1–11

2.2.2. Sentinel-1 Dataset

Sentinel-1 SAR data [40] is a global near-real-time dataset that helps monitor changes on the Earth's surface with great precision. It uses C-band radar, which means it can keep an eye on things and run continuously in any weather or light conditions, penetrating through clouds, vegetation, and harsh weather. For this study, we used VV and VH polarization data from the Sentinel-1 system.

These dual-polarization readings were especially useful in telling different types of surfaces apart and spotting changes in terrain. Our research looked at how the surface changed before and after fires, with a particular focus on how land and vegetation were affected. By measuring the spans in both the VV and VH bands, we were able to derive some key insights into the impact of fires on surface structures, which helped us better understand wildfire behavior.

2.2.3. Sentinel-2 Dataset

Sentinel-2 multispectral data [41] provides a great resource for assessing the effects of fires on vegetation. This dataset includes high-resolution red and near-infrared bands, which capture how vegetation reflects light. By calculating the NDVI, we can analyze vegetation health both before and after fire events to show the recovery of the vegetation after a fire event. Additionally, the Scene Classification Layer offers detailed information on various terrain types, which supports more comprehensive landscape analysis. These data enable daily monitoring of wildfire impacts on vegetation and provide valuable insights into ecosystem recovery. This is owing to the capability of Sentinel-2 imagery to map the burnt areas and assess severity. Furthermore, this information can be utilized for predictive modeling of future conditions.

2.3. Tools and Platform

This research uses Google Earth Engine (GEE) to facilitate the retrieval of geospatial data. This study has access to a wide range of public datasets and real-time information using a cloud-based platform. The primary purpose of the tool is to gather and display

extensive remote sensing data. In addition, ArcGIS was utilized to visualize TIFF files and produce maps. These tools have the capability to verify the accuracy of the data prior to conducting further analysis.

2.4. Wildfire Python Package

The Wildfire Python software package developed in this study greatly simplifies the computational notebook environment through automated data processing and wildfire prediction model integration. Everything from data pre-processing to data augmentation to the final predictive model is encapsulated in the package. Firstly, the package facilitates extensive processing and analysis of remotely sensed data and contains functions such as pre-processing in multispectral bands, fire score calculation, total power of synthetic aperture radar (SAR) data, and normalized vegetation index (NDVI) calculation. Secondly, the package is designed with a modular framework that supports a variety of deep learning frameworks, using GANS with TensorFlow to enhance data features and PyTorch for predictive modeling. This approach leverages the strengths of both platforms to optimize performance. TensorBoard is integrated into each module to enhance the user experience by providing powerful visualizations and efficient model tracking capabilities to easily monitor the training process and evaluate metrics.

For improved accessibility and easy integration into various projects, the package has been compiled into Wheel files (WHL) that can be directly installed and deployed. This feature makes it applicable not only to this study but also to other projects involving similar remote sensing data processing needs, highlighting its versatility and compatibility. The effectiveness and efficiency of the package have been demonstrated in this study, showing significant improvements in model performance and workflow optimization. Comprehensive documentation and example scripts are available on GitHub, allowing the research community to readily adapt and further develop the package.

2.5. Phase 1: Data Processing

2.5.1. Remote Sensing Data Band Processing

In this study, SNPP VIIRS and NOAA-20 VIIRS data were integrated to synthesize daily imagery and calculate fire scores (FS) using brightness temperatures (Bright-ti4, BT), confidence levels, and diurnal indicators (DayNight, DN). Confidence (C) was converted to a weighted scale (0.5, 1, 1.5) to reflect the level of certainty of detection, while DayNight was adjusted to take into account how the diurnal occurrence of fires affects human emergency response, e.g., for nighttime fires, the need to arrange for more attention during the night, which can often be easily overlooked. Taken together, these operations form a new layer dedicated to fire scoring in Equation (1).

$$FS = BT \times (0.5 \times C + 0.5) \times (2 \times DN - 1) \quad (1)$$

where Bright-ti4 is the brightness temperature in band 4, confidence is the confidence level, and DayNight indicates whether the observation was taken during the day (1) or night (0).

The second aspect of band processing involves Sentinel-1 GRD data, where the VV band provides intensity information from the surface that can reflect changes in the surface such as vegetation loss and soil exposure due to fire. The VH band, on the other hand, is sensitive to changes in vegetation structure and can reflect changes in vegetation height and density. Combining these two bands, according to the processing of the official GEE SAR data, this study calculates the total power image, which can be seen in Equation (2). This calculation is essential for assessing surface characteristics such as roughness and moisture. As these data are spliced from daily data sets with different locations at multiple time points, and there are days where there are no data in the study area, this study adopts

the use of the composite data as the underlying data and replaces the data where they are available to avoid the impact of missing values on the predictions.

$$\text{Span} = \text{VV2} + \text{VH2} \tag{2}$$

where VV represents the vertical–vertical polarization and VH represents the vertical–horizontal polarization.

For the Sentinel-2 SR Harmonized data, the SCL bands were extracted for scene classification, which has vegetation, saturated or defective areas, etc., which are important for prediction. In addition, the Normalized Vegetation Index (NDVI) was calculated using the red (B4) and near-infrared (B8) bands, the formula for which can be seen in Equation (3). This index is essential for monitoring vegetation health and assessing fire impacts. Again, to address data gaps and lack of coverage, we used the median of multi-day imagery to ensure consistency and accuracy of daily data. This integrated approach combines fire data with radar and multispectral imagery to form a new four-band dataset that clusters remotely sensed multi-source datasets and greatly improves the plausibility and accuracy of wildfire predictions.

$$\text{NDVI} = (\text{B8} - \text{B4})/(\text{B8} + \text{B4}) \tag{3}$$

where B8 represents the near-infrared band and B4 represents the red band.

2.5.2. Data Augmentation with GANs and Sliding Windows

The study found significant data deficiencies in the June and July fire data, as shown by the VIIRS bands. These gaps further complicated the processing of an already limited dataset. An important obstacle we faced was the requirement to forecast data for the month of August, which introduced an extra layer of complexity to the predictive modeling process. Upon analyzing meteorological data for the study area in 2024, a substantial alteration was seen in the climate compared to previous years. Nevertheless, August reverted to more customary circumstances [42]. In order to tackle this problem, the study utilized data from the months of November, December, January, and February, as the climatic and fire circumstances during these months closely resembled those of June and July. Subsequently, GANs were utilized to produce supplementary data for the months that were not available. The specific methodology is illustrated in Figure 1.

Furthermore, the study employed a sliding window data augmentation technique. This technique employs a sequence of seven photos, with each batch consisting of one set of photographs. The images are then moved backward one at a time, with each step being one unit. The sliding window's length was selected according to the requirement of forecasting fire data for the subsequent seven days. The selection of this strategy was based on the potential risk of losing crucial geographic details, which could have occurred if typical techniques like image rotation or cropping were employed.

Initially, the study starts by using a simple GAN model to create initial fire images. This model is made up of two parts: a generator and a discriminator. The generator takes random inputs from the latent space and turns them into images by passing them through several dense layers: a LeakyReLU activation layer, and a tanh layer at the end. The discriminator then checks these images to see if they are real or if they were created by the generator using a similar dense layer setup. This basic GAN setup helps to understand how GANs work and was used for the early image generation experiments in this study.

Based on the preliminary findings of SimpleGAN, this research showed that the outcomes of this model are not conducive to sparse data images such as fire. Consequently, SparseGAN was subsequently enhanced and refined. SparseGAN builds on the SimpleGAN framework by incorporating a sparsity loss function. This addition allows the

algorithm to produce sparser images that are better suited for specific image processing tasks, particularly in handling high-precision remote sensing data. The generator and discriminator architectures in SparseGAN are more complex and include the sparsity loss function, which helps to produce clearer and more recognizable images by eliminating unnecessary pixel activations. This reduces noise, enhances image quality, and makes the model more capable of handling difficult datasets.

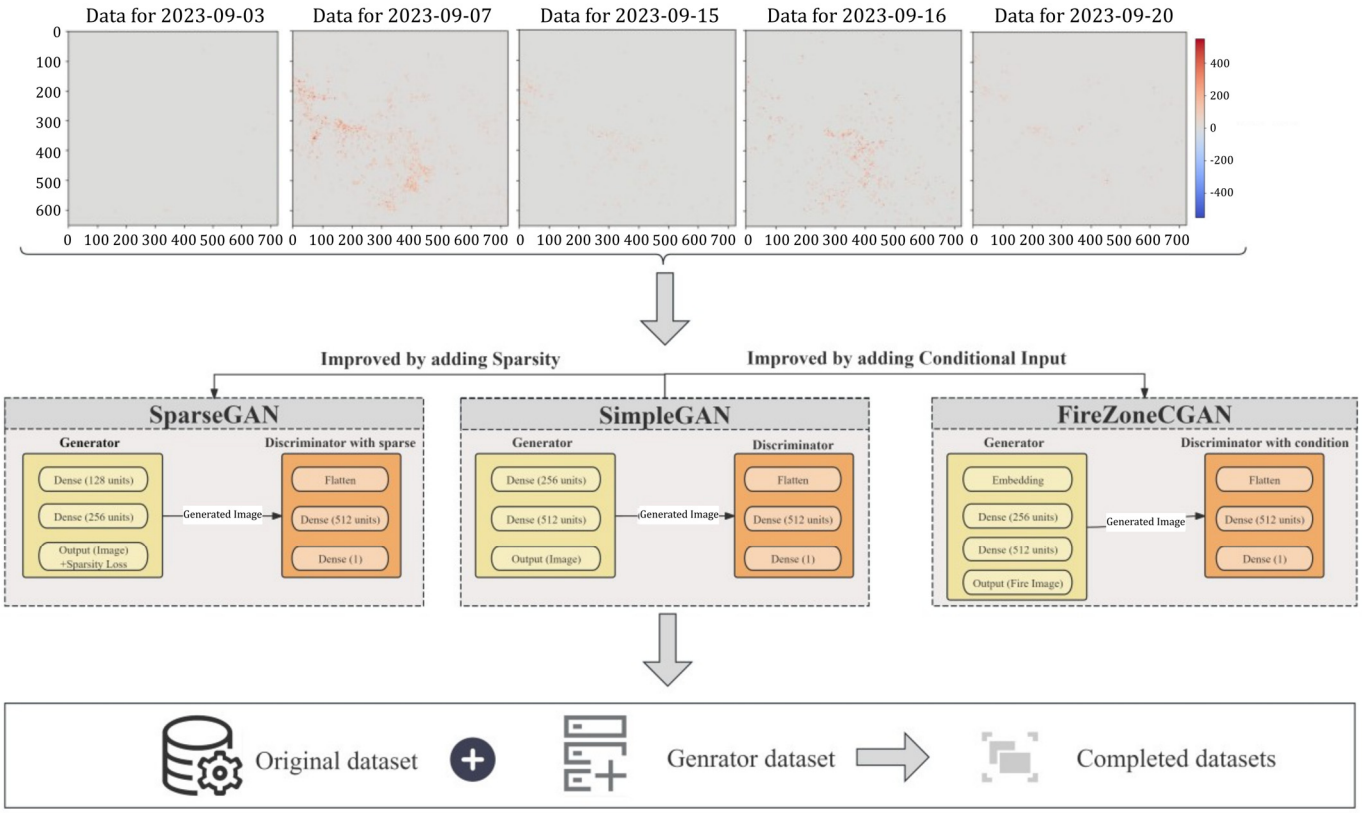

Figure 1. The structure of the Gans model and the technical route to improvement.

After analyzing the efforts made by SparseGAN, this study discovered that the introduction of sparse matrices resulted in some level of noise. As a result, FireZoneCGAN was implemented as an alternative approach. This model is a specialized adaptation of CGAN (conditional generative adversarial network) that produces images related to fire detection and analysis by taking certain inputs, such as the number of fire zones, into consideration [43,44]. It is extremely suitable for the process of generating realistic fire scenarios and enables more accurate fire predictions by simulating intricate surroundings and specific conditional controls. The generator utilizes input potential noise and condition labels to produce an image using a specified layer after embedding. The role of the discriminator is to assess these photographs and ascertain their authenticity. The FireZoneCGAN technique enhances the model's resilience to effectively mitigate a specific level of noise and improve the accuracy of fire data in scenarios characterized by limited patterns and sparse data [45].

2.6. Phase 2: Prediction Models

2.6.1. U-Net

In this study, the U-Net model is firstly used to process fire image data, especially to solve the time series problem with its high accuracy. U-Net is an encoder–decoder structured network that is widely used in image segmentation tasks and contains multiple convolutional blocks for performing downsampling and upsampling operations. This symmetric encoder–decoder architecture facilitates the precise detection of fire boundaries,

which is crucial information for accurate fire detection and monitoring. In other words, the U-Net model provides real-time processing of remote sensing data. Its image segmentation capability and multi-scale feature extraction structure make it well-suited for processing real-time image data, making it highly suitable for this research.

Throughout the model training process, the model processes the data independently at each time step, and the predictions correspond to the length of the time series. The output of each time step is generated using a specific convolutional layer and upsampling strategy, and the total model structure. The application order of this method, as well as the number of channels used, are shown in Figure 2. By monitoring the training process, optimizing parameter tuning, and performing analysis using TensorBoard, the performance and applicability of the model were significantly improved.

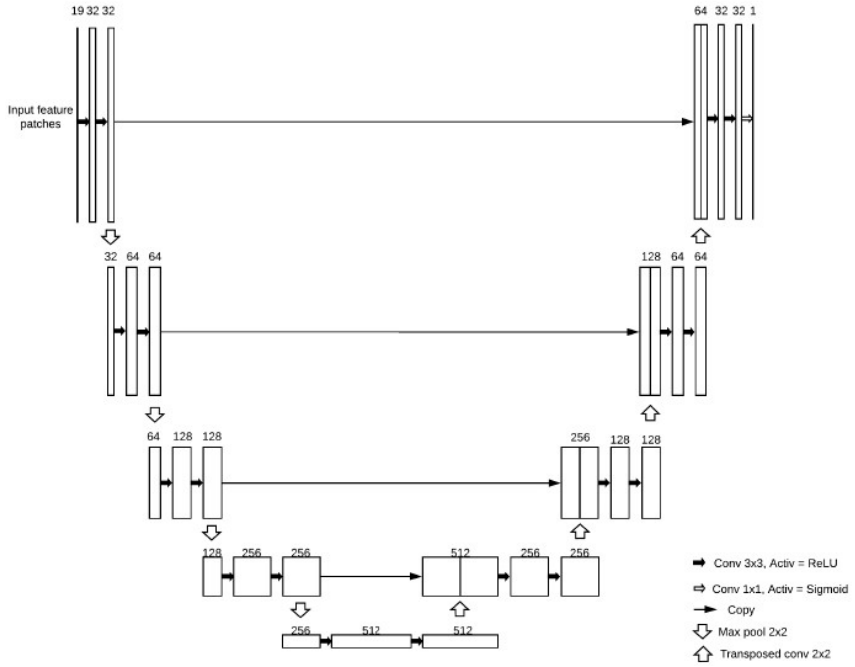

Figure 2. Employing U-Net for pixel-wise fire segmentation in images [46].

2.6.2. ConvLSTM

Apart from using U-Net in this study, a model of ConvLSTM is used to process fire image data associated with time series. These models combine CNN with LSTM and are empowered to effectively exploit the temporal processing power of a traditional LSTM combined with the spatial feature extraction power of a convolutional network, as shown in Figure A2. The ConvLSTM model would be very suitable to capture spatiotemporal dynamics in fire data, thereby making it ideal for managing such a complex dataset.

The extensive benefits of ConvLSTM in fire monitoring are that it can adapt well to dynamically changing environments and give highly accurate fire spread predictions. It is also likely to enable precision location (with the conditions of fire changes and in a very timely way) of fire-affected areas with high-resolution, remotely sensed data by processing both temporal and spatial information together. It will process each frame of the time series in sequence, thus continuous output will be generated from the model. In this way, a good foundation can be laid for later analyses and predictions of fire behavior.

In a nutshell, the ConvLSTM model improves the efficiency and accuracy of the treatment of fire image data and brings new methods and ways to handle complex spatio-temporal data with a deep learning architecture. The qualities mentioned make the ConvLSTM model an important component in this project, providing science and effectiveness for fire monitoring and management.

2.6.3. Attention ConvLSTM

Another innovative model was the Attention ConvLSTM model (model architecture shown in Figure A3), which combined the traditional network of ConvLSTM with a novel temporal attention mechanism that greatly enhanced its ability for dynamic analysis of environmental changes. Based on the effective ConvLSTM model, this innovative model provided the possibility of dynamically changing the attention of Attention ConvLSTM to different points in time by incorporating the mechanism of temporal attention, thereby optimizing the information flow and enhancing sensitivity to critical moments. With the attention mechanism integrated, it provides more accurate, sensitive recognition and prediction of fires against changes with time series, and strong support is possible for response to disasters in a timely manner and effective resource allocation. Moreover, this model, with its multi-layer structure and layer-by-layer information transfer design, further enhances the ability to capture subtle changes in high-resolution remote sensing data. These achievements not only demonstrate the strong potential of deep learning in spatiotemporal data analytics but also bring about a new, effective tool for fire monitoring and other related fields [47,48].

2.7. Phase 3: Train and Validation

The study employed FocalLoss to address the class imbalance, with the parameters $\alpha = 1.0$ and $\gamma = 2.0$. These values are optimal for reducing the dominance of well-classified examples and ensuring a focus on harder-to-classify instances, as discussed in Lin et al. [15]. The training was conducted with an adaptive learning rate of 0.0001, which was dynamically adjusted during training to avoid overfitting and improve convergence. Batch sizes of 16 and 8 were used based on the memory requirements of the models and the high dimensionality of the input data, similar to configurations suggested by Goodfellow et al. [49] for efficient training in high-dimensional feature spaces.

The study utilized a phased approach with 10-epoch cycles, repeated multiple times, to allow for intermediate validation and assessment without overwhelming computational resources. This phased approach aligns with best practice for model monitoring and debugging, as outlined by Zhang et al. [50], ensuring convergence while avoiding model degradation through overtraining.

During validation, regression accuracy was calculated by scaling outputs to the original data's range and assessing whether predictions fell within a tolerance level of 0.1, effectively evaluating the localized precision of predictions. This tolerance approach has been employed effectively in similar tasks involving geospatial predictions, as noted by Ban et al. [31], where localized error metrics are essential for high-precision applications like fire monitoring.

For benchmarking, parameters for baseline models, such as U-Net and ConvLSTM, were matched closely to ensure fairness. U-Net's encoder–decoder architecture leveraged multi-scale feature extraction for segmentation, aligning with Ronneberger et al. [51], while ConvLSTM adopted a temporal–spatial structure to effectively handle sequential data, as per Shi et al. [52].

3. Results

3.1. GANs

This study intensively trained and evaluated three different Generative Adversarial Network (GAN) models, namely SimpleGAN, SparseGAN, and CGAN, to assess their effectiveness in generating images of fire. The results in terms of images generated and loss plots are presented in Figure 3. These training processes have been adapted based on the optimal findings of related work that trained and used these models. 290 epochs

for SimpleGAN while 150 epochs for SparseGAN and CGAN have been implemented during model training due to sparsity constraints, conditional inputs, and remote sensing imagery necessitating different epochs for different GANs to achieve stable and realistic outputs [53–55].

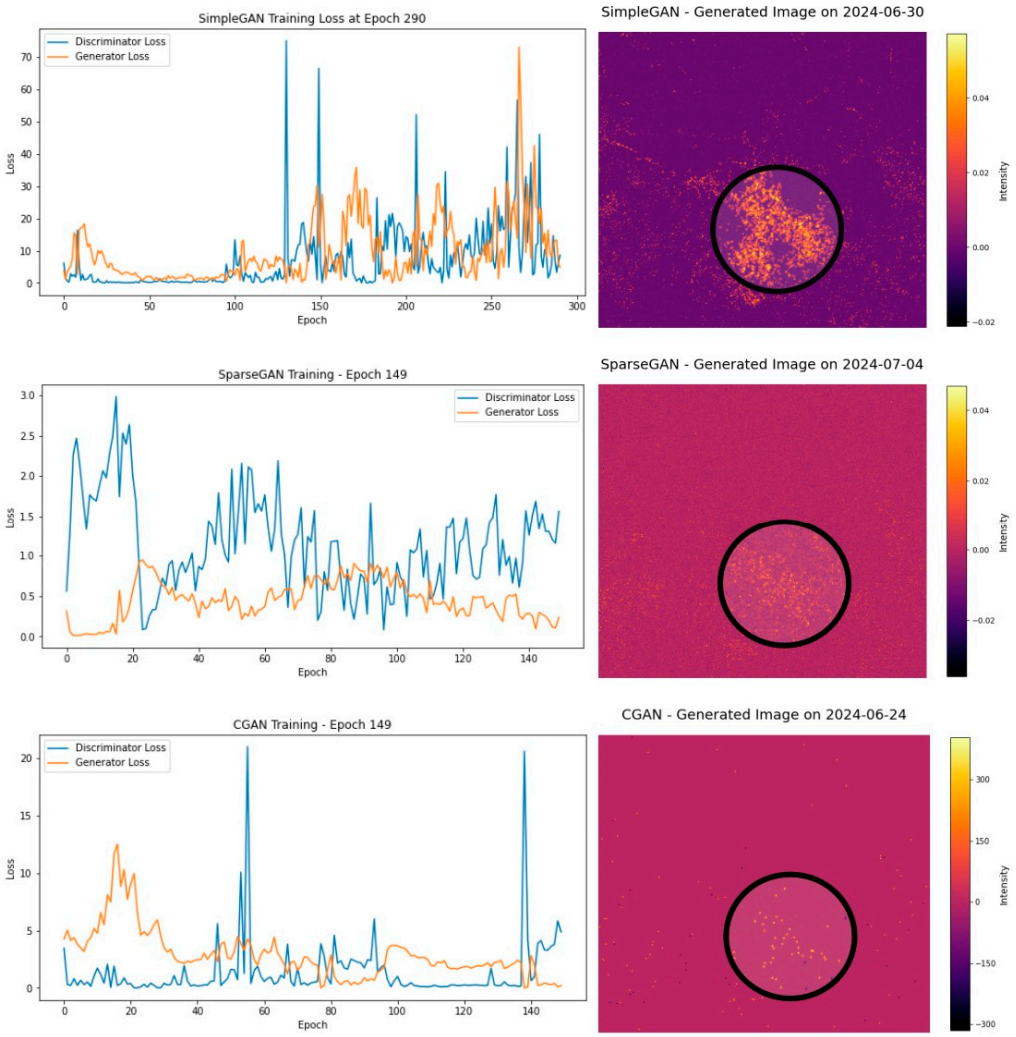

Figure 3. Loss plots and results of the GANs.

The training process of the SimpleGAN model exhibited significant fluctuations in loss value, highlighting the common challenges associated with GAN training stability. The plot features a few extreme loss values, which indicate instability despite some areas in the plot that showed a decrease in loss value. After 290 training epochs or complete passes through the training dataset, the image generated by SimpleGAN displayed some fire features that were concentrated in a few high-intensity regions. These attributes, however, lacked sufficient sparsity and adequate coverage of the actual areas affected by the fires. This outcome underscores the necessity of incorporating sparse matrices into the SimpleGAN model to enhance the processing of high-precision remote sensing data.

In contrast, SparseGAN demonstrated more stable loss values compared to SimpleGAN, indicating better control during training. After 150 epochs, SparseGAN was able to generate images with considerable consistency in the background, though it still struggled to accurately capture the complex features of fire, as many noise points persisted in the images. To improve this, we integrated conditional control within SparseGAN, allowing for more precise adjustments to the captured fire features and overall image quality.

Lastly, CGAN exhibited effective learning capabilities but experienced sharp spikes in loss values during certain periods depicted in Figure 3, primarily impacting the performance of the discriminator. This behavior suggests intense competition between the generator and discriminator. After 150 epochs, CGAN significantly improved the clarity and sparsity of fire points in its generated images, resulting in a cleaner background devoid of fire elements. This enhancement makes CGAN particularly valuable for fire monitoring applications. Given its superior performance and potential for generating practical and accurate images for fire monitoring, CGAN is positioned as the focal model for further research and application in this study, with the goal of refining image generation techniques to better support fire monitoring efforts.

3.2. Deep Learning Models

In the training of all three models, the value of Focal loss drops steadily while accuracy constantly rises, thus proving the models' efficacy and the final result shown in Table 2. For instance, the U-Net model was trained with a two percentage point decrease in loss that was followed by a corresponding two percentage point increase in stability and accuracy. However, due to the paucity of fire data, the reduction of loss did not increase along with accuracy; it was just a slow, progressive improvement. The prediction of fire events occurring during the next seven days (4 August to 11 August 2024), as shown in Figure 4, stated that while U-Net can predict the occurrence of fires, the generated images are not found to be particularly clear and sparse. There is still background noise present, but the relatively high concentration of fire points suggests that in some areas, the model's performance is much more effective.

Table 2. Comparison of model performance.

Model	Accuracy (%)	Focal Loss
U-Net	94.53	0.0059
ConvLSTM	95.85	0.0010

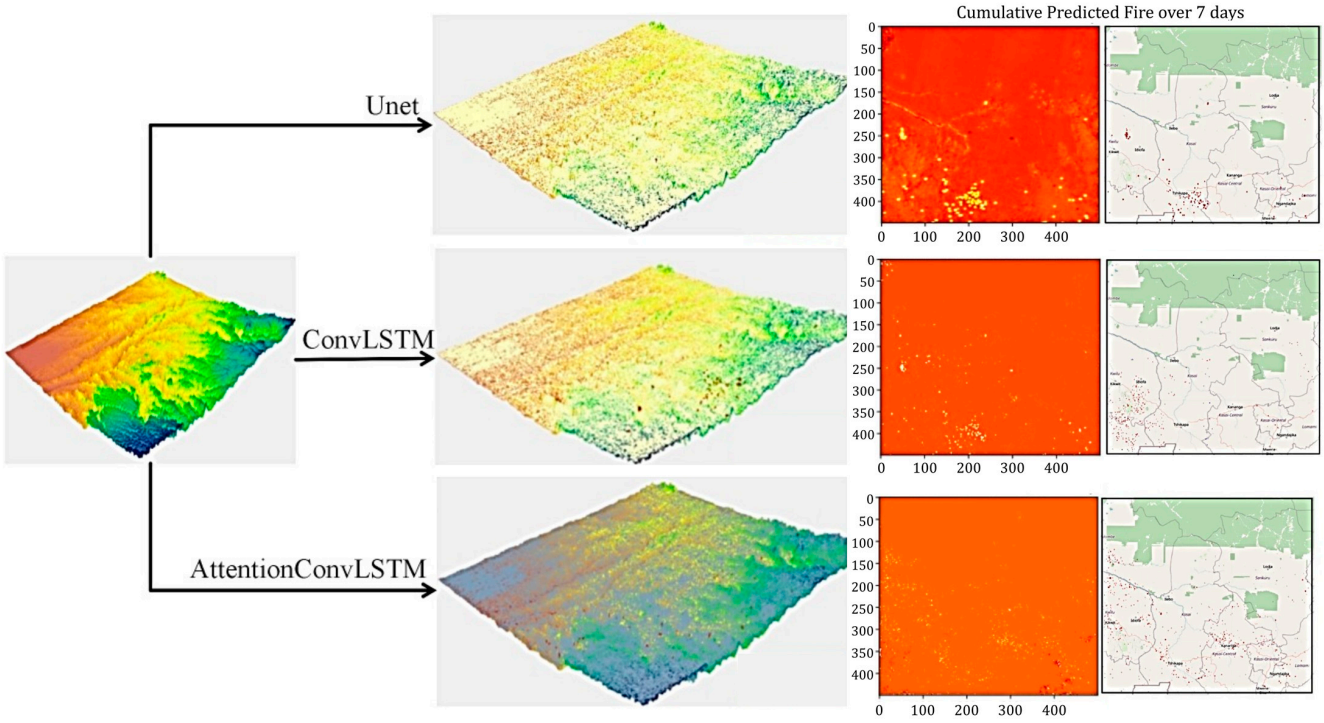

Figure 4. Prediction result of three models.

When compared with the accuracy of other deep learning models, the results of this study surpass the accuracy of other models such as the RCNN at 93.7% [19–21], SqueezeNet at 94.2% [22–24], and YOLOv5S and MobileNetV3 at 90.5% [25–27]. Moreover, the accuracy data is also on a par with the performance of CNN-based image processing methods at 96% accuracy [31,32] and just behind DCNN image segmentation and classification at 99.9% accuracy [28–30].

In terms of accuracy and best results in the reduction of loss, the ConvLSTM model presented this, and its training process also showed reliability in Figure 5. The clarity and sparsity of the generated fire images, along with the model, represented very close characteristics of the actual fire event distributions. Finally, Attention ConvLSTM, which builds above ConvLSTM, is slightly suboptimal in its accuracy but promising, especially with hard temporal data.

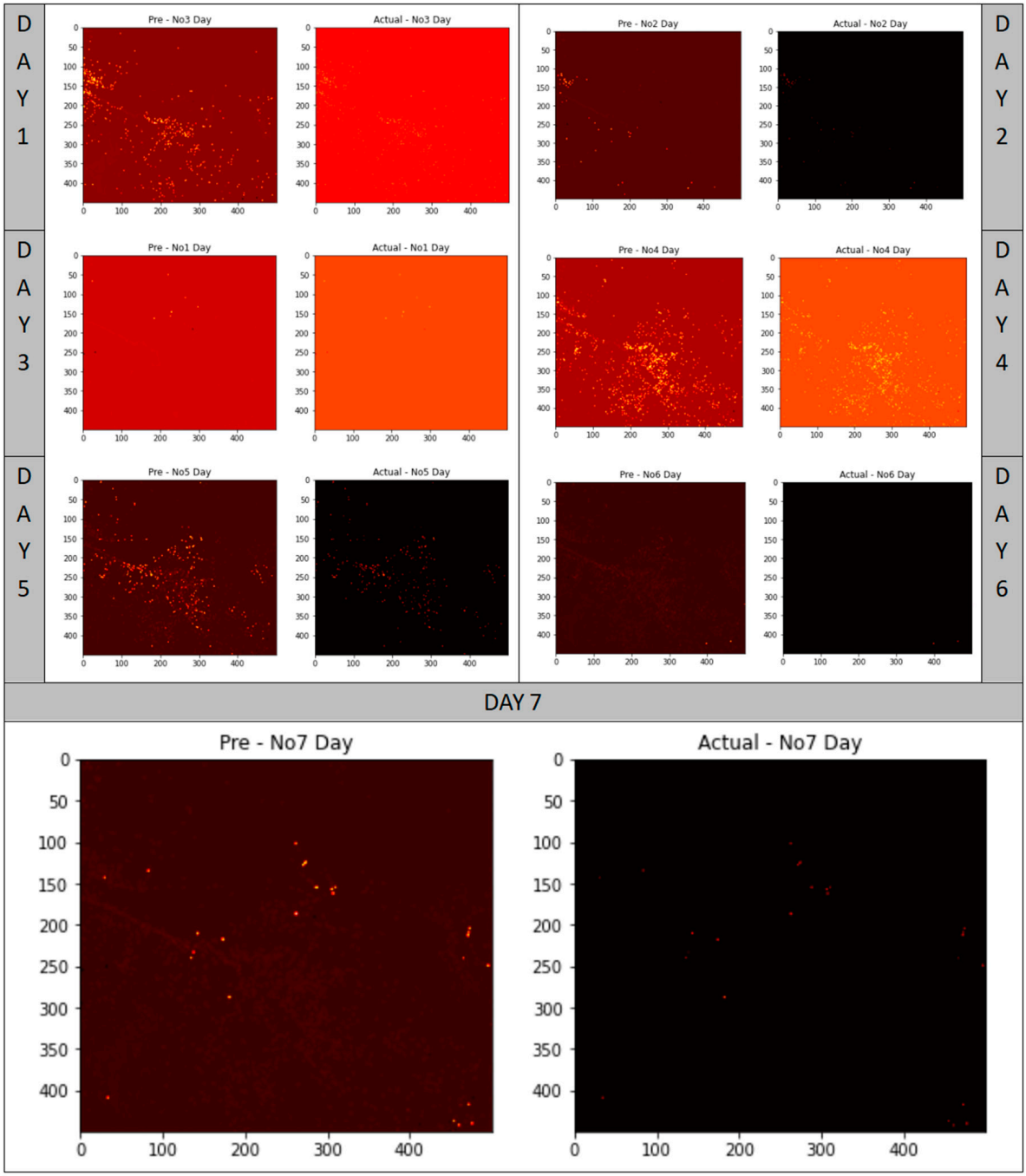

Figure 5. The training process of the ConvLSTM model shows reliability.

4. Discussion and Conclusions

This study determined that the novel application of sliding windows for data augmentation significantly enhanced model accuracy in the context of real-time remote sensing data processing and fire area prediction. Moreover, CGANs exhibited superior performance in managing sparse data, which is prevalent in fire prediction. This finding indicates that GAN data generation should be task-specific rather than solely emphasizing diverse metrics and the rivalry between the generator and the discriminator. In all predictive models, ConvLSTM has shown enhanced performance regarding time efficiency and outcomes, underscoring its efficacy in managing fire prediction time series data. This underscores the model's efficacy in addressing the sparsity issue with fire data. Furthermore, U-Net and Attention ConvLSTM attained significant accuracy, illustrating their efficacy in processing high-resolution remotely sensed data and time series data. The study, which focuses on the Congo region, also underscored the need to choose a suitable study area with adequate validation data. The initial usage of Landsat data significantly compromised the prediction outcomes due to substantial cloud occlusion; thus, data selection and processing are crucial components of deep learning and picture segmentation tasks. The introduction of novel methodologies and building on existing research strategies and data led to improvement in the accuracy of deep learning models, as demonstrated by the analysis of current research trends. This study was able to yield data accuracy significantly greater than existing studies and has the potential to compete with the accuracy that DCNN image segmentation and classification offers at 99.9%. The key element of integrating deep learning with remote sensing data is the understanding and pre-processing of the extensive volume of remote sensing data, signifying a pioneering effort in this field.

However, there were several limitations of the study related to model biases, dataset constraints, temporal and spatial applicability, and synthetic data augmentation. The first limitation is that the ConvLSTM and Attention ConvLSTM models may be prone to overfitting specific features of the dataset and study area despite their high accuracy [49,50]. As for the reliance on the VIIRS and Sentinel datasets, they are limited in terms of data gaps and cloud cover interference, albeit these limitations are common in satellite-based fire monitoring [56,57]. Moreover, there may be inaccuracies in the use of GAN-based augmentation techniques to address data sparsity. With regards to the region selected for the study, the model may not perform as effectively in regions with different seasonal patterns or fire dynamics as in the Republic of the Congo, with its distinct dry and wet seasons. Addressing these limitations in future studies by incorporating diverse datasets, additional geographic regions, and enhanced data validation techniques could improve model robustness and broaden the applicability to wildfire prediction and monitoring. Nevertheless, the model can be perpetually refined by integrating supplementary training data via this technical process as part of future initiatives. This will facilitate the model's training for forecasting future fires. The entire procedure can be finalized within one day and can predict regions susceptible to fire hotspots for the following seven days. Furthermore, after the reliable model is stored, real-time forecasts can be generated. The developed framework, function packages, and models, being advanced wireless sensor networks, are not limited to this specific application only. They may also be extended to include further forms of high-precision remote sensing data processing, high-resolution image processing, and various transdisciplinary applications, such as in processing medical data and images. This facilitates a wider array of interdisciplinary applications. Lastly, an important future direction to further the findings of this study is in the integration of real-life data for the verification of the model's effectiveness and feasibility of the processing method employed.

Author Contributions: Conceptualization, M.S. and S.Y.; data curation, S.Y.; formal analysis, S.Y.; investigation, S.Y.; methodology, M.S. and S.Y.; project administration, M.S.; resources, M.S.; supervision, M.S.; writing—original draft, S.Y.; writing—review and editing, M.S. All authors have read and agreed to the published version of the manuscript.

Funding: This research received no external funding.

Informed Consent Statement: Not applicable.

Data Availability Statement: The VIIRS and Sentinel datasets for this study can be accessed at https://drive.google.com/drive/folders/1Xx3GzmNeHfG5zvXI_g5LErTCI0hRiJfm?usp=sharing (accessed on 29 December 2024.)

Acknowledgments: The authors are grateful for the support of the Center for Environmental Policy at Imperial College London.

Conflicts of Interest: The authors declare no conflicts of interest.

Appendix A

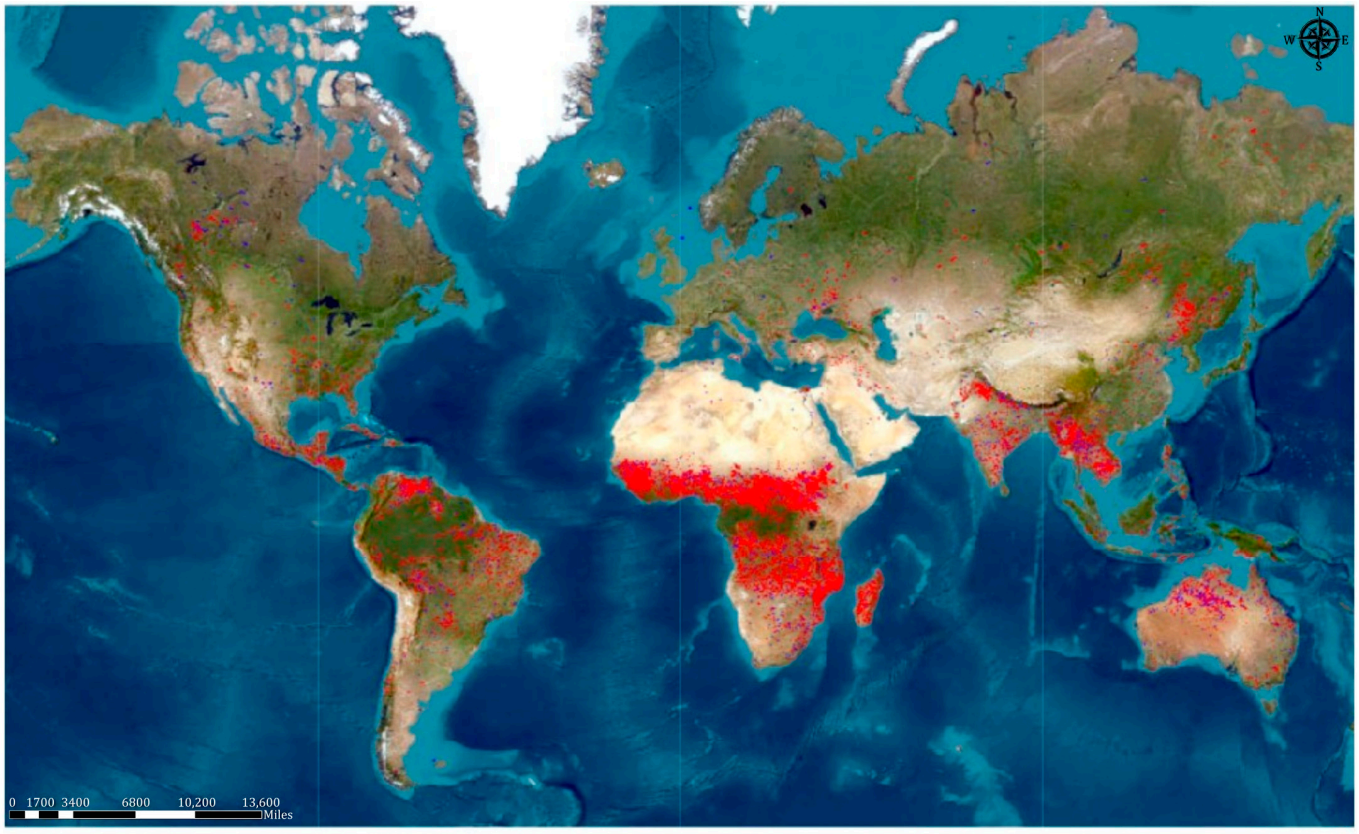

Figure A1. Global VIIRS fire visualization.

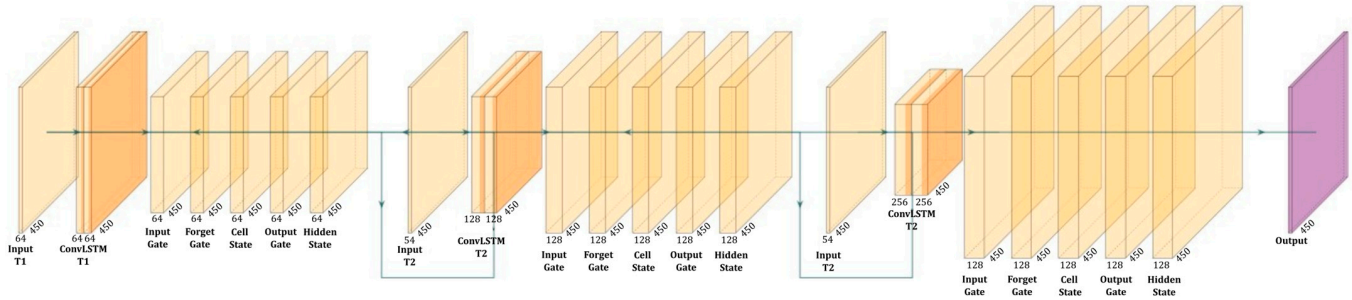

Figure A2. Structure of the customized ConvLSTM model plotted with PlotNeuralNet.

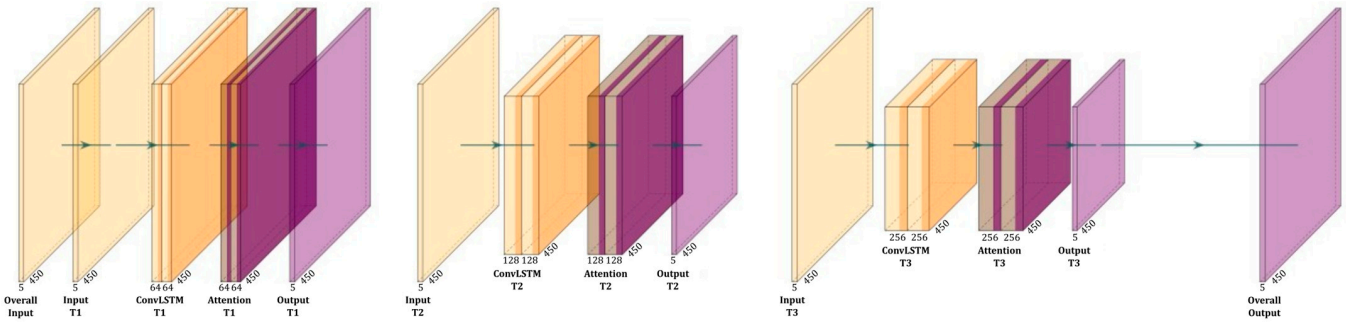

Figure A3. Structure of the customized Attention ConvLSTM model plotted with PlotNeuralNet.

References

1. Zheng, Y.; Zhang, G.; Tan, S.; Feng, L. Research on Progress of Forest Fire Monitoring with Satellite Remote Sensing. *Agric. Rural. Stud.* **2023**, *1*, 8. [CrossRef]
2. Chan, X.; Liu, L.; Li, J.; Ou, W.; Zhang, Y. Application and research progress of fire monitoring using satellite remote sensing. *Natl. Remote Sens. Bull.* **2020**, *24*, 531–542. [CrossRef]
3. Xiao-rui, T.; Mcrae, D.J.; Li-fu, S.; Ming-yu, W.; Hong, L. Satellite remote-sensing technologies used in forest fire management. *J. For. Res.* **2005**, *16*, 73–78. [CrossRef]
4. Kim, Y.; Kim, B.-R.; Park, S. Synergistic use of multi-satellite remote sensing to detect forest fires: A case study in South Korea. *Remote Sens. Lett.* **2023**, *14*, 491–502. [CrossRef]
5. Alexeeff, S.E.; Liao, N.S.; Liu, X.; Van Den Eeden, S.K.; Sidney, S. Long-Term PM 2.5 Exposure and Risks of Ischemic Heart Disease and Stroke Events: Review and Meta-Analysis. *J. Am. Heart Assoc.* **2020**, *10*, e016890. [CrossRef]
6. Liang, F.; Liu, F.; Huang, K.; Yang, X.; Li, J.; Xiao, Q.; Chen, J.; Liu, X.; Cao, J.; Shen, C.; et al. Long-Term Exposure to Fine Particulate Matter and Cardiovascular Disease in China. *J. Am. Coll. Cardiol.* **2020**, *75*, 707–717. [CrossRef]
7. Wang, Y.; Eliot, M.N.; Wellenius, G.A. Short-term Changes in Ambient Particulate Matter and Risk of Stroke: A Systematic Review and Meta-analysis. *J. Am. Heart Assoc.* **2014**, *3*, e000983. [CrossRef]
8. Finlay, S.E.; Moffat, A.; Gazzard, R.; Baker, D.; Murray, V. Health impacts of wildfires. *PLoS Curr.* **2012**, *4*, e4f959951cce2c. [CrossRef]
9. Grant, E.; Runkle, J.D. Long-term health effects of wildfire exposure: A scoping review. *J. Clim. Change Health* **2022**, *6*, 100110. [CrossRef]
10. Gao, Y.; Huang, W.; Yu, P.; Xu, R.; Yang, Z.; Gasevic, D.; Ye, T.; Guo, Y.; Li, S. Long-term impacts of non-occupational wildfire exposure on human health: A systematic review. *Environ. Pollut.* **2023**, *320*, 121041. [CrossRef]
11. Walding, N.G.; Williams, H.T.P.; McGarvie, S.; Belcher, C.M. A comparison of the US National Fire Danger Rating System (NFDRS) with recorded fire occurrence and final fire size. *Int. J. Wildland Fire* **2018**, *27*, 99–113. [CrossRef]
12. Freeborn, P.H.; Cochrane, M.A.; Jolly, W.M. Relationships between fire danger and the daily number and daily growth of active incidents burning in the northern Rocky Mountains, USA. *Int. J. Wildland Fire* **2015**, *24*, 900–910. [CrossRef]
13. McFayden, C.B.; George, C.; Johnston, L.M.; Wotton, M.; Johnston, D.; Sloane, M.; Johnston, J.M. A case-study of wildland fire management knowledge exchange: The barriers and facilitators in the development and integration of the Canadian Forest Fire Danger Rating System in Ontario, Canada. *Int. J. Wildland Fire* **2022**, *31*, 835–846. [CrossRef]
14. Alkhatib, A.A.A. A Review on Forest Fire Detection Techniques. *Int. J. Distrib. Sens. Netw.* **2014**, *10*, 597368. [CrossRef]
15. Lin, Z.; Chen, A.; Wang, X.; Liu, Z.; Piao, S. Large language models reveal big disparities in current wildfire research. *Commun. Earth Environ.* **2024**, *5*, 168. [CrossRef]
16. Joshi, J.; Sukumar, R. Improving prediction and assessment of global fires using multilayer neural networks. *Sci. Rep.* **2021**, *11*, 3295. [CrossRef]
17. Phelps, L.N.; Andela, N.; Gravey, M.; Davis, D.S.; Kull, C.A.; Douglass, K.; Lehmann, C.E.R. Madagascar's fire regimes challenge global assumptions about landscape degradation. *Glob. Change Biol.* **2022**, *28*, 6944–6960. [CrossRef]
18. Joseph, G.S.; Seymour, C.L.; Rakotoarivelo, A.R. Fire incongruities can explain widespread landscape degradation in Madagascar's forests and grasslands. *Plants People Planet* **2024**, *6*, 656–669. [CrossRef]
19. Xie, F.; Huang, Z. Aerial forest fire detection based on transfer learning and improved faster RCNN. In Proceedings of the 2023 IEEE 3rd International Conference on Information Technology, Big Data and Artificial Intelligence (ICIBA), Chongqing, China, 26–28 May 2023.
20. Zhang, L.; Wang, M.; Fu, Y.; Ding, Y. A forest fire recognition method using UAV images based on transfer learning. *Forests* **2022**, *13*, 975. [CrossRef]

21. Wang, W.; Huang, Q.; Liu, H.; Jia, Y.; Chen, Q. Forest fire detection method based on deep learning. In Proceedings of the 2022 International Conference on Cyber-Physical Social Intelligence (ICCSI), Nanjing, China, 18–21 November 2022.
22. Wang, G.; Zhang, Y.; Qu, Y.; Chen, Y.; Maqsood, H. Early forest fire region segmentation based on deep learning. In Proceedings of the 2019 Chinese Control And Decision Conference (CCDC), Nanchang, China, 3–5 June 2019.
23. Ghali, R.; Akhloufi, M.A.; Jmal, M.; Mseddi, W.S.; Attia, R. Forest fires segmentation using deep convolutional neural networks. In Proceedings of the 2021 IEEE International Conference on Systems, Man, and Cybernetics (SMC), Melbourne, Australia, 17–20 October 2021.
24. Kong, S.; Deng, J.; Yang, L.; Liu, Y. An attention-based dual-encoding network for fire flame detection using optical remote sensing. *Eng. Appl. Artif. Intell.* **2024**, *127*, 107238. [CrossRef]
25. Wei, C.; Xu, J.; Li, Q.; Jiang, S. An intelligent wildfire detection approach through cameras based on deep learning. *Sustainability* **2022**, *14*, 15690. [CrossRef]
26. Hongyu, H.; Ping, K.; Li, F.; Huaxin, S. An improved multi-scale fire detection method based on convolutional neural network. In Proceedings of the 2020 17th International Computer Conference on Wavelet Active Media Technology and Information Processing (ICCWAMTIP), Chengdu, China, 18–20 December 2020.
27. Xue, Q.; Lin, H.; Wang, F. Fcdm: An improved forest fire classification and detection model based on yolov5. *Forests* **2022**, *13*, 2129. [CrossRef]
28. Ghali, R.; Akhloufi, M.A.; Mseddi, W.S. Deep learning and transformer approaches for UAV-based wildfire detection and segmentation. *Sensors* **2022**, *22*, 1977. [CrossRef] [PubMed]
29. Ghali, R.; Akhloufi, M.A.; Jmal, M.; Mseddi, W.S.; Attia, R. Wildfire segmentation using deep vision transformers. *Remote Sens.* **2021**, *13*, 3527. [CrossRef]
30. Ghali, R.; Akhloufi, M.A. Deep learning approaches for wildland fires remote sensing: Classification, detection, and segmentation. *Remote Sens.* **2023**, *15*, 1821. [CrossRef]
31. Ban, Y.; Zhang, P.; Nascetti, A.; Bevington, A.R.; Wulder, M.A. Near real-time wildfire progression monitoring with Sentinel-1 SAR time series and deep learning. *Sci. Rep.* **2020**, *10*, 1322. [CrossRef]
32. Toan, N.T.; Cong, P.T.; Hung, N.Q.V.; Jo, J. A deep learning approach for early wildfire detection from hyperspectral satellite images. In Proceedings of the 2019 7th International Conference on Robot Intelligence Technology and Applications (RiTA), Daejeon, Republic of Korea, 1–3 November 2019.
33. Gonzalez, J.A.C.; Perez, K.D.J.R.; Barros, T.; Corso, G.F.; Araújo, J.M.D. A Comparison of U-Net with Conditional Generative Adversarial Networks and Cycle-Consistent Adversarial Networks for real seismic data interpolation: Tupi Field. *Res. Soc. Dev.* **2024**, *13*, e1613746226. [CrossRef]
34. Quintana-Quintana, O.J.; De León-Cuevas, A.; González-Gutiérrez, A.; Gorrostieta-Hurtado, E.; Tovar-Arriaga, S. Dual U-Net-Based Conditional Generative Adversarial Network for Blood Vessel Segmentation with Reduced Cerebral MR Training Volumes. *Micromachines* **2022**, *13*, 823. [CrossRef]
35. Pérez, M.R.; de Blas, D.E.; Nasi, R.; Sayer, J.A.; Sassen, M.; Angoué, C.; Gami, N.; Ndoye, O.; Ngono, G.; Nguinguiri, J.-C.; et al. Logging in the Congo Basin: A multi-country characterization of timber companies. *For. Ecol. Manag.* **2005**, *214*, 221–236. [CrossRef]
36. Bösch, M. Institutional quality, economic development and illegal logging: A quantitative cross-national analysis. *Eur. J. For. Res.* **2021**, *140*, 1049–1064. [CrossRef]
37. Nasi, R.; Billand, A.; van Vliet, N. Managing for timber and biodiversity in the Congo Basin. *For. Ecol. Manag.* **2012**, *268*, 103–111. [CrossRef]
38. NASA LANCE: SNPP VIIRS C2 Dataset. 3 September 2023. Available online: https://developers.google.com/earth-engine/datasets/catalog/NASA_LANCE_SNPP_VIIRS_C2 (accessed on 1 October 2024).
39. NASA LANCE: NOAA-20 VIIRS C2 Dataset. 8 October 2023. Available online: https://developers.google.com/earth-engine/datasets/catalog/NASA_LANCE_NOAA20_VIIRS_C2 (accessed on 1 October 2024).
40. COPERNICUS S1 GRD Dataset. 3 October 2014. Available online: https://developers.google.com/earth-engine/datasets/catalog/COPERNICUS_S1_GRD (accessed on 1 October 2024).
41. COPERNICUS S2 SR HARMONIZED Dataset. 28 March 2017. Available online: https://developers.google.com/earth-engine/datasets/catalog/COPERNICUS_S2_SR_HARMONIZED (accessed on 1 October 2024).
42. Average Weather in Democratic Republic of the Congo. 31 December 2016. Available online: https://zh.weatherspark.com/countries/CD (accessed on 1 October 2024).
43. Mirza, M.; Osindero, S. Conditional generative adversarial nets. *arXiv* **2014**, arXiv:1411.1784.
44. Dash, A.; Ye, J.; Wang, G. A Review of Generative Adversarial Networks (GANs) and Its Applications in a Wide Variety of Disciplines: From Medical to Remote Sensing. *IEEE Access* **2024**, *12*, 18330–18357. [CrossRef]
45. Radford, A. Unsupervised representation learning with deep convolutional generative adversarial networks. *arXiv* **2015**, arXiv:1511.06434.

46. McCarthy, N.; Tohidi, A.; Aziz, Y.; Dennie, M.; Valero, M.; Hu, N. A deep learning approach to downscale geostationary satellite imagery for decision support in high impact wildfires. *Forests* **2021**, *12*, 294. [CrossRef]
47. Cao, S.; Feng, D.; Liu, S.; Xu, W.; Chen, H.; Xie, Y.; Zhang, H.; Pirasteh, S.; Zhu, J. BEMRF-Net: Boundary Enhancement and Multiscale Refinement Fusion for Building Extraction From Remote Sensing Imagery. *IEEE J. Sel. Top. Appl. Earth Obs. Remote Sens.* **2024**, *17*, 16342–16358. [CrossRef]
48. Xie, Y.; Zhan, N.; Zhu, J.; Xu, B.; Chen, H.; Mao, W.; Luo, X.; Hu, Y. Landslide extraction from aerial imagery considering context association characteristics. *Int. J. Appl. Earth Obs. Geoinf.* **2024**, *131*, 103950. [CrossRef]
49. Goodfellow, I.; Bengio, Y.; Courville, A. *Deep Learning*; MIT Press: Cambridge, MA, USA, 2016.
50. Zhang, A.; Lipton, Z.; Li, M.; Smola, A. *Dive into Deep Learning*; Cambridge University: Cambridge, UK, 2021.
51. Ronneberger, O.; Fischer, P.; Brox, T. U-Net: Convolutional Networks for Biomedical Image Segmentation. In *Medical Image Computing and Computer-Assisted Intervention—MICCAI 2015*; Springer International Publishing: New York City, NY, USA, 2015; pp. 234–241.
52. Shi, X.; Chen, Z.; Wang, H.; Yeung, D.-Y.; Wong, W.-K.; Woo, W.-C. Convolutional LSTM network: A machine learning approach for precipitation nowcasting. *Adv. Neural Inf. Process. Syst.* **2015**, *28*.
53. Goodfellow, I.; Pouget-Abadie, J.; Mirza, M.; Xu, B.; Warde-Farley, D.; Ozair, S.; Bengio, Y. Generative Adversarial Nets. *Adv. Neural Inf. Process. Syst.* **2014**.
54. Chen, Y.; Ma, L.; Wen, C.; Li, Y. Sparse Convolutional Neural Networks. *IEEE Trans. Pattern Anal. Mach. Intelligance* **2018**, *40*, 2994–3006.
55. Pan, Z.; Zhang, L.; Li, L.; Wu, F. Learning to Augment Data with Conditional GAN for Remote Sensing Image Classification. *Remote Sens.* **2019**, *11*.
56. Roy, D.; Boschetti, L.; Justice, C.; Ju, J. The collection 5 MODIS burned area product—Global evaluation by comparison with the MODIS active fire product. *Remote Sens. Environ.* **2015**, *112*, 3690–3707. [CrossRef]
57. Justice, C.O.; Giglio, L.; Korontzi, S.; Owens, J.; Morisette, J.T.; Roy, D.; Descloitres, J.; Alleaume, S.; Petitcolin, F.; Kaufman, Y. MODIS Fire Products. *Remote Sens. Environ.* **2002**, *83*, 244–262. [CrossRef]